JOURNAL OF SOLID STATE CHEMISTRY **123,** 161–167 (1996)
ARTICLE NO. 0164

Nonstoichiometry and Physical Properties of the Two Dimensional $Sr_{1+x}Nd_{1-x}FeO_{4-y}$ System

Min Gyu Kim, Kwang Hyun Ryu, and Chul Hyun Yo

Department of Chemistry, Yonsei University, Seoul 120-749, Korea

Received January 30, 1995; in revised form January 23, 1996; accepted January 29, 1996

The compounds $Sr_{1+x}Nd_{1-x}FeO_{4-y}$ ($x = 0.00, 0.25, 0.50, 0.75,$ and 1.00) with the K_2NiF_4 structure are prepared by a drip pyrolysis technique. X-ray powder diffraction analysis assigns all the compositions to the tetragonal system with decreasing lattice volume as x increases. Nonstoichiometric chemical formulas are formulated and identified by Mohr salt analysis and Mössbauer spectroscopy, respectively. Oxygen vacancy formation is predominant rather than the oxidation of the Fe^{3+} ion to the Fe^{4+} ion with respect to the competitive compensation for the positive charge deficiency. The electrical and magnetic properties of these compounds, with the space group *I*4/*mmm*, are different from those of the corresponding three-dimensional perovskites. All the compositions of the two-dimensional $Sr_{1+x}Nd_{1-x}FeO_{4-y}$ compounds are within the semiconducting range with positive temperature dependence of the electrical conductivity. Although the amount of Fe^{4+} ion is maximum at the composition of $x = 1.00$, its lowest electrical conductivity can be associated, not with the conduction carrier concentration, but with the mobility which depends on the amount of the oxygen vacancy and on the Fe–O–Fe bond distance. As a result of the magnetic measurement with a SQUID, all the compositions follow the Curie–Weiss law and the anomalous effective magnetic moments of the compositions can be interpreted as a coexistence of low and high spins of the mixed valence state.

INTRODUCTION

The structure and physical properties of nonstoichiometric perovskite-related compounds, ABO_{3-y} (A = rare earth elements, B = transition metals), with three-dimensional characteristics have been studied extensively. The electrical and magnetic properties of nonstoichiometric perovskites with the general formula $A_{1-x}A'_xBO_{3-y}$ have been described as the result of the degree of B–O–B interaction, the structural distortion leading to the specific electronic configuration of the B cation, and the mixed valence state of B cations and oxygen vacancies occurring when a divalent A' ion is substituted for the trivalent A ion (1 ~ 5).

The study for the Mössbauer resonance spectra of the $SrFeO_{3-\delta}$ system with a wide range of nonstoichiometry has shown the mixed valence of Fe cations and the distorted site arising from the presence of an oxygen vacancy. Gibb (1) and Fournés *et al.* (2) have reported that $SrFeO_{2.75}$ solid solution is composed of the Fe^{3+} ion in octahedral sites and the Fe^{4+} ion with high spin configuration stabilized by a highly distorted site and that $SrFeO_{2.83}$ compound has average $Fe^{3.5+}$ valence state implying a short range hopping. The electrical conductivities of these nonstoichiometric perovskites have been investigated by the amount of Fe^{4+} ion, the influences of the oxygen vacancy, and also the mobility of conduction carriers which decrease with the increase of the Fe–O–Fe average distance according to the hopping conduction model. Hombo *et al.* (3) have shown that the mobility of conduction carriers rather than the carrier density decreases largely with the increase of the oxygen vacancies.

The representative K_2NiF_4-type compounds have tetragonal structures with the *I*4/*mmm* space group which is composed of the interlayers of the rock salt within the perovskite layers. Therefore, it can be anticipated that the oxygen nonstoichiometry may be the main factor for characteristics of the K_2NiF_4-type compounds, similar to their corresponding perovskites. Because of the relatively weak interplanar interactions along the c axis between the magnetic ions in K_2NiF_4-type compounds (4), the differences of structural and physical properties between these compounds and corresponding perovskites would be expected. The structural study for the $A_{0.5}La_{1.5}Li_{0.5}Fe_{0.5}O_4$ (A = Ca, Sr, Ba) system by Demazeau *et al.* (5–7) has shown that the more covalent character of the Fe–O bond than the Li–O bond causes the D_{4h} distortion of FeO_6 octahedra. This strong D_{4h} elongation is sufficient to stabilize the d_{z^2} orbital and leads to the high spin configuration of the Fe^{4+} ion.

The relatively large quadrupole splitting (ΔE_q = 1.28 ~ 0.99 mm/s) presented in the Mössbauer spectroscopic study at 300 K by Fournés *et al.* (8) has shown not only the octahedral site distortion but also the anisotropic electronic configuration ($d^1_{xz}d^1_{yz}d^1_{xy}d^1_{z^2}d^0_{x^2-y^2}$) of the Fe^{4+} ion. The degree of the structural distortion can also be repre-

0022-4596/96 $18.00

sented as the tetragonality (c/a) which means the degree of elongation of oxygen octahedra along the c axis and the stabilization of the high spin configuration of the Fe ion in $c/a = 3.36 \sim 3.47$ (5–7).

The preparation and characterization of K_2NiF_4-type compounds with stoichiometric compositions have been studied previously (9–11). In the present study, the influences of the structure, the mixed valency of the Fe ion, and the oxygen vacancy on the electrical and magnetic properties for the nonstoichiometric $Sr_{1+x}Nd_{1-x}FeO_{4-y}$ system will be investigated.

EXPERIMENTAL

Spectroscopic pure powders of $SrCO_3$, Nd_2O_3, and $Fe(NO_3)_3 \cdot 9H_2O$ are used as starting materials for the preparation of $Sr_{1+x}Nd_{1-x}FeO_{4-y}$ compounds. The solid solutions with the composition range $0.00 \leq x \leq 1.00$ have been prepared by dripping the mixture of appropriate stoichiometric starting materials initially dissolved in dilute nitric acid into the hot quartz tube at 800°C in an electrical furnace. After being ground, the mixture is heated at 900°C under air atmosphere for 24 h and quickly quenched to room temperature. The grinding and heat treatment are repeated in order to prepare the homogeneous nonstoichiometric solid solution.

X-ray diffraction patterns are obtained with monochromated Cu$K\alpha$ radiation ($\lambda = 1.5418$ Å) using a Philips PW-1710 X-ray diffractometer. The lattice parameters and crystal system are determined from least-square fits of the diffraction lines indexed with the tetragonal space group $I4/mmm$ for all the compositions. The oxidation states of Fe ions are specified by chemical analysis in which the reduction of the Fe^{4+} ion into the Fe^{3+} ion by the Mohr salt is followed by the redox titration for excess Fe^{2+} ion with standard potassium dichromate solution. Nonstoichiometric chemical formulas of the $Sr_{1+x}Nd_{1-x}FeO_{4-y}$ system for all the compositions have been determined.

Mössbauer resonance spectra are obtained with a ^{57}Co/Rh source at room temperature. Mössbauer spectroscopic analysis has been accomplished by the curve fitting with Lorentzian function.

Electrical conductivities of the compounds have been measured by four probe dc method in the temperature range from 170 K to room temperature. Voltages and currents are measured independently with a Keithley Model 236 Source Measure Unit (SMU) under evaporating liquid nitrogen. The electrical conductivities are calculated using Laplume's equation (12). The magnetic susceptibilities are measured after they approached the thermal equilibrium along zero field cooling with the Superconducting Quantum Interference Device (SQUID) from 4 K to room temperature.

RESULTS AND DISCUSSION

The X-ray diffraction analyses for the $Sr_{1+x}Nd_{1-x}FeO_{4-y}$ system assigned tetragonal symmetry of the representative K_2NiF_4-type structure for all the compositions. The lattice parameters, the lattice volumes of unit cell, and the tetragonalities (c/a) for all the compositions are listed in Table 1.

In the composition range from $x = 0.00$ to 0.50, as x value increases, lattice parameter a decreases to be minimized and c increases to be maximized at $x = 0.50$, respectively. However the lattice parameters for a composition range from $x = 0.50$ to 1.00 have a reverse tendency against those of the above composition range. As larger Sr^{2+} ions are substituted for Nd^{3+} ions in 9-coordinated sites, the tetragonality (c/a) in the lattice structure increases to be maximized at $x = 0.50$, which means the elongation of oxygen octahedra along the c axis is maximum at the composition. However, in the composition range from $x = 0.50$ to 1.00, the tetragonality decreases with the increasing x value up to minimum at $x = 1.00$.

The lattice parameters can be associated with the electronic configuration of the transition elements and the physical properties of the low-dimensional characteristic metal oxides. The correlation between the A–O apical distance in rock salt layer or the B–O apical distance of the BO_6 octahedra in $(A'A)_2BO_4$ and the sizes of the inserted A' cations has been described by Labbe *et al.* (13). The substituted Sr^{2+} ion is randomly distributed between perovskite layers and rock salt layers in the $Sr_{1+x}Nd_{1-x}FeO_{4-y}$ system with the low Sr^{2+} concentration. However, the more increase in Sr^{2+} concentration causes the dorminant occupancy of the Sr^{2+} ion into rock salt layers rather than the Nd^{3+} ion. Thus the largest tetragonality at $x = 0.50$ may be explained as the dominant site occupancy of the Sr^{2+} ion within rock salt layers.

In K_2NiF_4-type compounds, it has been generally suggested that the interplanar interactions between magnetic ions along the c axis are very weak due to the presence of rock salt layers compared with the intraplanar interactions within the ab planes. The distances between (110), (200),

TABLE 1
Lattice Parameters, Unit Cell Volume, and Tetragonality for the $Sr_{1+x}Nd_{1-x}FeO_{4-y}$ System

x value	Lattice parameter (Å)		Unit cell volume (Å^3)	Tetragonality c/a
	a	c		
0.00	3.846(9)	12.618(4)	186.75(4)	3.28
0.25	3.833(2)	12.624(9)	185.50(2)	3.29
0.50	3.829(3)	12.636(1)	185.28(2)	3.30
0.75	3.839(9)	12.564(2)	185.27(3)	3.27
1.00	3.866(7)	12.136(3)	181.45(4)	3.14

TABLE 2
τ, y Values and Nonstoichiometric Chemical Formula for the $Sr_{1+x}Nd_{1-x}Fe^{3+}_{1-\tau}Fe^{4+}_{\tau}O_{4-y}$ System

x value	τ value	y value	Nonstoichiometric chemical formula
0.00	0.09 (±0.004)	−0.04(5)	$SrNdFe^{3+}_{0.91}Fe^{4+}_{0.09}O_{4.04}$
0.25	0.10 (±0.003)	0.07(5)	$Sr_{1.25}Nd_{0.75}Fe^{3+}_{0.90}Fe^{4+}_{0.10}O_{3.93}$
0.50	0.12 (±0.004)	0.19(3)	$Sr_{1.50}Nd_{0.50}Fe^{3+}_{0.88}Fe^{4+}_{0.12}O_{3.81}$
0.75	0.14 (±0.003)	0.30(5)	$Sr_{1.75}Nd_{0.25}Fe^{3+}_{0.86}Fe^{4+}_{0.14}O_{3.70}$
1.00	0.31 (±0.003)	0.34(5)	$Sr_2Fe^{3+}_{0.69}Fe^{4+}_{0.31}O_{3.66}$

and (220) planes among the *hkl* planes indexed from X-ray diffraction patterns, as it will be shown later, can be used as the standards for the degree of interaction between magnetic ions in the *ab* plane.

Table 2 shows the mole ratio of Fe^{4+} ions to total Fe ions or the τ value obtained from the chemical analysis, the amount of oxygen vacancies or y value, and the nonstoichiometric chemical formula for all the compositions. The competitive formation of the oxygen vacancies and the Fe^{4+} ions can compensate for the positive charge deficiency due to the substitution of the Sr^{2+} ion in place of the Nd^{3+} ion. As shown in Fig. 1, the formation of the oxygen vacancy is dominant rather than that of Fe^{4+} ions for the compositions of $x \geq 0.25$ in the $Sr_{1+x}Nd_{1-x}FeO_{4-y}$ system. For the perovskite $Nd_{1-x}Sr_xFeO_{3-y}$ system, it is reported that the formation of Fe^{4+} ions is prior to that of oxygen vacancies (14). These tendencies can be interpreted that the substitution of the large Sr^{2+} ion leads to the easier coordination with 12-oxygen anions than the small Nd^{3+} ion. So this fact results in the large formation of Fe^{4+} ions in the corresponding perovskite. Because the difference between the ionic radii of the Sr^{2+} and Nd^{3+} ions has little influence on the coordination with 9-oxygen anions in the $Sr_{1+x}Nd_{1-x}FeO_{4-y}$ system, the formation of oxygen vacancies is dominant.

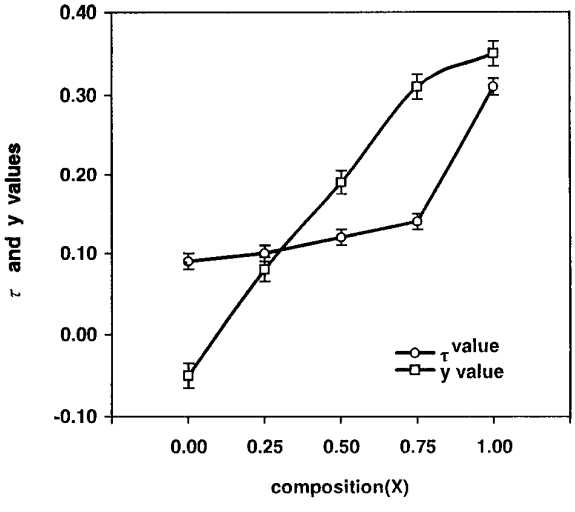

FIG. 1. The plots of the τ (mole ratio of Fe^{4+} ions to total Fe ions) and y values for the $Sr_{1+x}Nd_{1-x}FeO_{4-y}$ system.

Takano *et al.* (15) reported the relationship between the lattice parameter and the oxygen vacancy in the $SrFeO_{3-\delta}$ system. Since the oxygen vacancies cause the electrostatic repulsive force between the Fe cations and the cations are pushed apart, the lattice parameter increases with increasing oxygen vacancies. The lattice parameters in this system, therefore, can be used as a standard to estimate the more dominant distribution of the oxygen vacancies among the rock salt layers and the perovskite layers. It was found that the distributions of oxygen vacancies for the compositions $x = 0.25$ and 0.50 in the $Sr_{1+x}Nd_{1-x}FeO_{4-y}$ system are dominant along the c axis rather than in the *ab* plane and for the compositions $x = 0.75$ and 1.00 are dominant in the *ab* plane rather than along the c axis. It is reasonable that this system has the dependence of oxygen vacancy distribution on the preferred direction.

The ^{57}Fe Mössbauer resonance spectra for the solid solutions recorded at room temperature are shown in Fig. 2. All the spectra are asymmetric due to the existence of more than one oxidation state of the Fe ions. The Mössbauer parameters such as isomer shift (δ) and quadrupole splitting (ΔE_q) are listed in Table 3. The observed linewidths are broader than those natural for the γ-ray (14.4 keV) emitted from the source ^{57}Co, which shows the system may be disordered at room temperature (15). All the spectra do not show any magnetic hyperfine splitting at room temperature. The magnetic ordering temperature must be below the room temperature.

Two quadrupole doublets of $x = 0.00$ are compatible with the Fe^{3+} and Fe^{4+} ions in the octahedral sites, respectively. For the compositions $x = 0.25$ and 1.00, the third quadrupole doublet can be interpreted as arising from the tetrahedral sites of Fe^{3+} ions. There is a large correlation between the isomer shift of the Fe^{4+} ion and the covalency of the Fe^{4+}–O bond, in addition to the neighboring Fe^{3+}–O bonding covalency. The strong covalency of the Fe^{4+}–O bond induced by π bonding between Fe t_{2g} orbitals and O 2_p orbitals decreases the shielding effect on s electrons. As a result, the s electron density at the nucleus is larger due to back donation of t_{2g} electrons into π ligand orbitals. Therefore, the decrease of the Fe–O–Fe bond distance shifts the isomer shift of the Fe^{4+} ion to a more negative value. This fact presents that the small Fe–O–Fe bond distance in the *ab* plane corresponds to the large negative isomer shift of the Fe^{4+} ion, as shown in $x = 0.25$ and 0.50. Also, the strong covalency of the Fe^{4+}–O bond weakens the covalency of the Fe^{3+}–O bond intersecting an intermediate oxygen anion. A small isomer shift of the Fe^{4+} ion shows a large one of the Fe^{3+} ions in the octahedral sites in good agreement with Table 3.

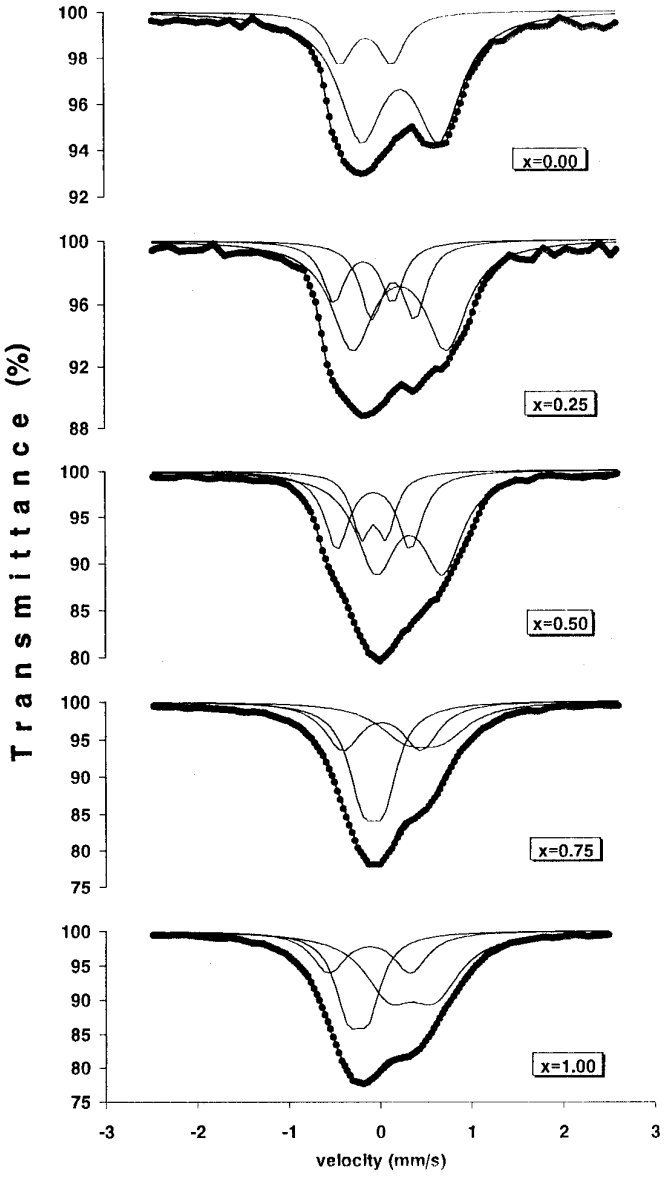

FIG. 2. Mössbauer spectra of the $Sr_{1+x}Nd_{1-x}FeO_{4-y}$ system at room temperature.

It was found that the quadrupole splitting of the Fe^{4+} ion seems to have a linear relation to the tetragonality. Especially the difference between the quadrupole splitting for the Fe^{4+} ion of $Sr_2FeO_{3.66}$ in this system and that of Sr_2FeO_4 (17) can be explained as tetragonalities, because the larger tetragonality indicates the larger structural distortion by the elongation of oxygen octahedra.

The plots of log electrical conductivity as a function of $1000/T$ present a good linearity at the low temperature region as shown in Fig. 3. The activation energies for the electrical conduction are listed in Table 4. All the two-dimensional $Sr_{1+x}Nd_{1-x}FeO_{4-y}$ compounds show semiconducting behavior with positive temperature dependence of the electrical conductivity. In many perovskites, it has been explained mainly by the hopping conduction mechanism that the activation energy depends on the amount of the Fe^{4+} ion which can form a $3d$ hole as a conduction carrier. However, the electrical conductivity in this system is not proportional to the amount of Fe^{4+} ions. Although the

TABLE 3
Mössbauer Parameters for the $Sr_{1+x}Nd_{1-x}FeO_{4-y}$ System at Room Temperature

x value	Component	δ^a	$\Delta E_q{}^b$	Γ^c	Area (%)
0.00	Fe^{3+}(Oh)	0.29(6)	0.87(9)	0.65(4)	89.1
	Fe^{4+}(Oh)	−0.11(1)	0.54(4)	0.50(4)	11.9
0.25	Fe^{3+}(Oh)	0.37(2)	0.88(6)	0.56(8)	65.7
	Fe^{3+}(Td)	0.05(9)	0.78(3)	0.48(4)	19.5
	Fe^{4+}(Oh)	−0.16(5)	0.65(6)	0.59(3)	14.8
0.50	Fe^{3+}(Oh)	0.38(3)	0.75(2)	0.59(9)	61.3
	Fe^{3+}(Td)	0.11(2)	0.58(2)	0.48(1)	20.5
	Fe^{4+}(Oh)	−0.16(9)	0.60(4)	0.48(5)	18.2
0.75	Fe^{3+}(Oh)	0.24(2)	0.42(5)	0.58(9)	54.1
	Fe^{3+}(Td)	0.04(1)	0.42(9)	0.57(3)	24.3
	Fe^{4+}(Oh)	0.01(3)	0.15(9)	0.66(1)	21.3
1.00	Fe^{3+}(Oh)	0.31(7)	0.37(9)	0.53(2)	49.9
	Fe^{3+}(Td)	0.03(9)	0.56(2)	0.59(6)	25.7
	Fe^{4+}(Oh)	−0.05(9)	0.11(5)	0.55(1)	24.4

[a] δ, isomer shift (mm/s).
[b] ΔE_q, quadrupole splitting (mm/s).
[c] Γ, line width (mm/s).

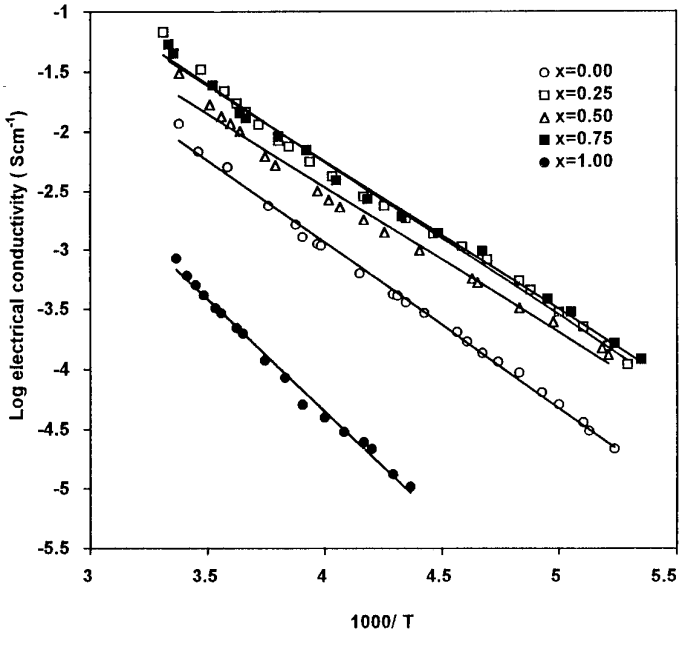

FIG. 3. Plots of log electrical conductivity as a function of $1000/T$ for the $Sr_{1+x}Nd_{1-x}FeO_{4-y}$ system.

TABLE 4
Activation Energy for the Electrical Conduction in the $Sr_{1+x}Nd_{1-x}FeO_{4-y}$ System

x value	Activation energy (eV)
0.00	0.27(7)
0.25	0.25(8)
0.50	0.24(5)
0.75	0.25(1)
1.00	0.37(2)

composition $x = 1.00$ contains the largest amount of Fe^{4+} ions over all the compositions, the activation energy for electrical conduction is the largest. This inconsistent result can be illustrated based on the study of Hombo *et al.* (3) that the concentration of conduction carriers is independent of the temperature at the low temperature range as a result of the temperature independence of the Seebeck coefficient.

The conductivities in low temperature depend on the degree of Fe–O–Fe interaction and the amount of oxygen vacancies within the lattice. The relationships of the electrical conductivity with the lattice parameter and the oxygen vacancy can elucidate this point. As shown in Fig. 4, the activation energy change on the composition is similar to the change of average distances between (110), (200), and (220) planes representing the degree of Fe–O–Fe interaction. Finally it is concluded that the electrical conductivities of the $Sr_{1+x}Nd_{1-x}FeO_{4-y}$ compounds are associated with not the conduction carrier concentration itself or τ value but conduction carrier mobility which depends on the oxygen vacancy and the distance between the Fe cations.

Inverse magnetic susceptibilities as a function of temperature in a temperature range from 4 to 300 K are shown in Fig. 5. All the compositions of the $Sr_{1+x}Nd_{1-x}FeO_{4-y}$ system follow Curie–Weiss behavior. Magnetic exchange in perovskite compounds generally takes place by the superexchange interaction which occurs between magnetic ions via the nearest neighboring oxygen anion and gives rise to an antiferromagnetic coupling. As shown in Table 5, the paramagnetic Curie temperatures, θ_p, increase with x value due to the random distribution of the Fe^{4+} ions. The positive θ_p value at $x = 1.00$ can be possibly interpreted as the short range ordering of ferromagnetic Fe^{4+}–O–Fe^{3+} interaction caused by the higher concentration of the Fe^{4+} ion but interrupted abruptly by the oxygen vacancy.

The spin only effective magnetic moments of the Fe ions are obtained on the assumption that the Nd^{3+} ion with total angular magnetic moment of 3.62 μ_B in the ground state $^4I_{9/2}$ has no magnetic interaction with the Fe cations. Thus, the effective magnetic moment of only Fe ions at $x = 0.00$ and the others cannot be specified as the low spin or high spin state.

The two interpretations are possible about these anomalous effective magnetic moments. The first is the coexistence of the low and high spins for the Fe^{3+} and Fe^{4+} ions distributed randomly over the materials. Second, the intermediate electronic configuration between the Fe^{3+} ($d^1_{xz}d^1_{yz}d^1_{xy}d^1_{z^2}d^1_{x^2-y^2}$) ion and the Fe^{4+} ($d^1_{xz}d^1_{yz}d^1_{xy}d^1_{z^2}d^0_{x^2-y^2}$) ion would be expected. In the case of the latter interpretation, the calculated effective magnetic moment, 3.69 μ_B, for $x = 0.00$ approximates to the empirical one, 3.35 μ_B, for $x = 0.00$.

However, the linewidth in the Mössbauer resonance spectra is too broad to characterize the intermediate electronic configurations of the Fe^{3+} and Fe^{4+} ions. Since the tetragonalities in this system ($c/a = 3.17 \sim 3.30$) are smaller than those in the K_2NiF_4-type compounds ($c/a =$

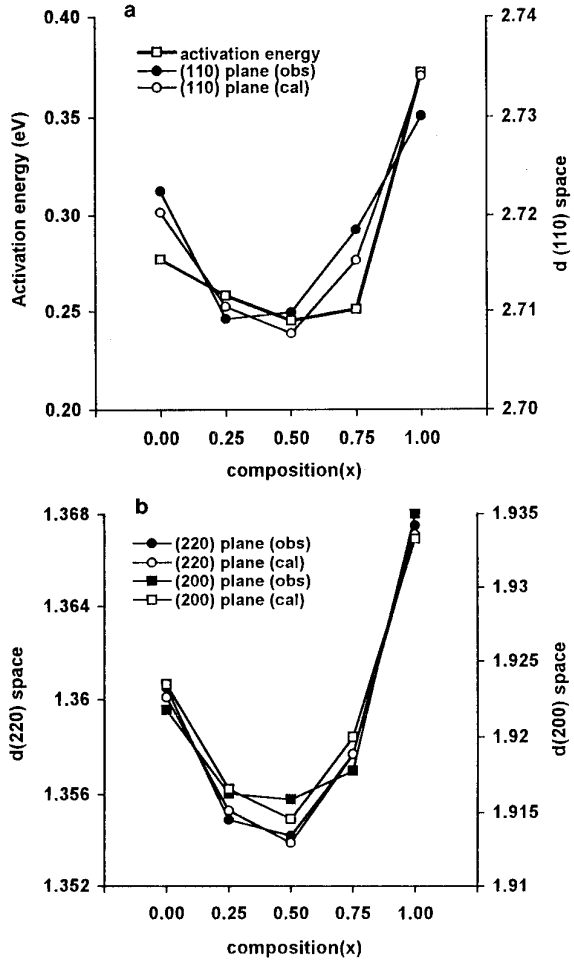

FIG. 4. (a) Plots of the activation energy for the electrical conduction and the calculated and observed distances (dimension of Å) between (110) planes. (b) Plots of the calculated and observed distances between (200) and (220) planes.

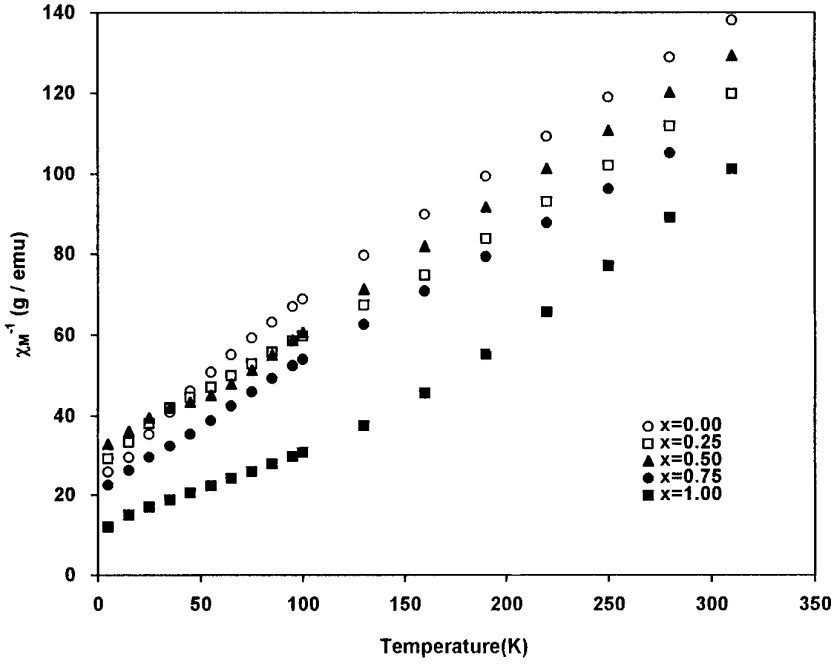

FIG. 5. Plots of χ_M^{-1} as a function of temperature for the $Sr_{1+x}Nd_{1-x}FeO_{4-y}$ system.

3.36 ~ 3.47) which are sufficient to stabilize a high spin state for the Fe ion, it may be suggested that the high and low spins of the Fe ions in this system should be mixed together with the appropriate ratio.

CONCLUSION

The $Sr_{1+x}Nd_{1-x}FeO_{4-y}$ system with tetragonally symmetric structure has two-dimensional characteristics in physical properties which depend on atomic arrangements in the *ab* plane rather than along the *c* axis. The substitution of the Sr^{2+} ion in place of the Nd^{3+} ion results in the more predominant formation of the oxygen vacancy rather than that of Fe^{4+} ions and the distribution of oxygen vacancies depends on the directions. The distribution of the oxygen vacancies and the Fe–O–Fe bond distance play important roles in the electrical conductivity of $Sr_{1+x}Nd_{1-x}FeO_{4-y}$ system. The oxygen vacancy and the weak overlap between Fe 3*d* orbitals and O 2*p* orbitals weaken the transfer of conduction carrier to neighboring Fe ions. The Jahn–Teller distortion generally shown in compounds with K_2NiF_4 structure is relatively small in the $Sr_{1+x}Nd_{1-x}FeO_{4-y}$ system, which cannot specify only the high spin state of the Fe^{4+} ion. The large oxygen vacancies and two-dimensional magnetic coupling give rise to decreasing the magnetic ordering temperature. As shown in the effective magnetic moments, the Fe ions have low and high spin states in the system together.

TABLE 5
Paramagnetic Curie Temperature, Total Effective Magnetic Moment, and Spin Only Effective Magnetic Moment of the Fe Ion for the $Sr_{1+x}Nd_{1-x}FeO_{4-y}$ System

Composition	θ_p(K)	$\mu_{eff}(\mu_B)$	μ_{eff}(Fe)(μ_B)
0.00	−111.9	4.93	3.35
0.25	−107.7	5.29	4.27
0.50	−86.2	4.93	4.22
0.75	−89.8	5.31	4.99
1.00	+40.7	4.64	4.64

ACKNOWLEDGMENTS

This work was supported by Grant 92-25-00-02 from the Korea Science and Engineering Foundation in 1993 and therefore we express our appreciation to the authorities concerned.

REFERENCES

1. T. C. Gibb, *J. Chem. Soc. Dalton Trans.* 1455 (1985).
2. L. Fournés, Y. Potin, J. C. Grenier, G. Demazeau, and M. Pouchard, *Solid State Commun.* **62**(4), 239 (1987).
3. J. Hombo, Y. Matsumoto, and T. Kawano, *J. Solid State Chem.* **84,** 138 (1990).
4. G. Le Flem, G. Demazeau, and P. Hagenmuller, *J. Solid State Chem.* **44,** 82 (1982).
5. G. Demazeau, M. Pouchard, N. Chevreau, J. F. Colombet, M. Thomas, F. Menil, and P. Hagenmuller, *J. Less Common Metals* **76,** 279 (1980).

6. G. Demazeau, B. Buffat, M. Pouchard, and P. Hagenmuller, *J. Solid State Chem.* **54,** 389 (1984).
7. G. Demazeau, L. M. Zhu, L. Fournés, M. Pouchard, and P. Hagenmuller, *J. Solid State Chem.* **72,** 31 (1988).
8. L. Fournés, G. Demazeau, L. M. Zhu, N. Chevreau, and M. Pouchard, *Hyperfine Interact.* **53**(1–4), 335 (1990).
9. M. Vlasse, M. Perrin, and G. Le Flem, *J. Solid State Chem.* **32,** 1 (1980).
10. J. L. Soubeyroux, P. Courbin, L. Fournès, D. Fruchart, and G. Le Flem, *J. Solid State Chem.* **31,** 313 (1980).
11. C. N. R. Rao, P. Ganguly, K. K. Singh, and R. A. M. Ram, *J. Solid State Chem.* **72,** 14 (1988).
12. J. Laplume, *L'onde Electrique* **35,** 113 (1955).
13. Ph. Labbe, M. Ledesert, V. Caignaert, and B. Raveau, *J. Solid State Chem.* **91,** 362 (1991).
14. C. H. Yo, H. R. Kim, K. H. Ryu, K. S. Roh, and J. H. Choy, *Bull. Korean Chem. Soc.* **15**(8), 636 (1994).
15. M. Takano, Y. Takeda, and J. B. Goodenough, *J. Solid State Chem.* **73,** 140 (1988).
16. T. C. Gibb, P. D. Battle, S. K. Bollen, and R. J. Whitehead, *J. Mater. Chem.* **2**(1), 111 (1992).
17. S. E. Dann, M. T. Weller, D. B. Currie, M. F. Thomas, and A. D. Al-Rawwas, *J. Mater. Chem.* **3**(12), 1231 (1993).